Accepted Manuscript

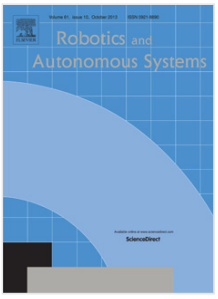

A novel tele-operation controller for wireless microrobots in-pipe with hybrid motion

Jian Guo, Shuxiang Guo, Xiang Wei

PII: S0921-8890(15)00153-0
DOI: http://dx.doi.org/10.1016/j.robot.2015.07.009
Reference: ROBOT 2505

To appear in: *Robotics and Autonomous Systems*

Received date: 19 November 2014
Revised date: 8 March 2015
Accepted date: 9 July 2015

Please cite this article as: J. Guo, S. Guo, X. Wei, A novel tele-operation controller for wireless microrobots in-pipe with hybrid motion, *Robotics and Autonomous Systems* (2015), http://dx.doi.org/10.1016/j.robot.2015.07.009

A Novel Tele-operation Controller for wireless Microrobots in-pipe with Hybrid Motion

Jian Guo [a], Shuxiang Guo [a, b] and Xiang Wei [a]

[a] Tianjin Key Laboratory for Control Theory and Application in Complicated Systems and Biomedical Robot Laboratory, Tianjin University of Technology, Tianjin, China

[b] Intelligent Mechanical Systems Engineering Department, Kagawa University, Takamatsu, Japan

Abstract

Intracavity intervention is expected to become more and more popular in the medical practice, both for diagnosis and for surgery. Wireless microrobots are employed in a wide range of biomedical application, they have many potential to accomplish many medical procedures radically, which is due to they can be carried deeply within the body of living organisms to perform tasks safe and reliable. The method of colonoscopy is an important procedure for the diagnosis of various pathologies, especially in cancer of the colon and rectum. However, it is often painful to the patient and complex to the doctor during the colonoscopy process, so the wireless microrobots have been very necessary for early diagnosis of malignant tumor in gastrointestine (GI). In this paper, a novel tele-operation system which would be used in the biomedical application has been proposed, and the master controller and slaver controller in the system had been designed. We also designed a novel kind of wireless microrobot with hybrid motion which driven by the different external magnetic field. The doctor could operate the joysticks from the master side to control the wireless microrobot in slave side in real time. With the control algorithm of 8-Steps rotation magnetic field, the slave controller could generate a more uniform rotation magnetic field and avoided many problems that occurring in traditional control method. Based on some experiments, the performance between the tele-operated controller and the wireless microrobot with hybrid motion had been evaluated. The experimental results indicated that the wireless microrobot with hybrid motion could complete forward-backward, upward-downward motion easily with the similar kinematic characteristics, and the available frequency band would be widened with the control algorithm of 8-Steps rotation magnetic field. Besides that, the maximum velocity could be measured at 29.8 mm/s round 18 Hz in the horizontal direction and 9.6 mm/s round 16 Hz in the vertical direction with input current of 0.7 A. The tele-controller showed a good performance in the experiments and it would be widely used in medical clinic in the future.

Research highlights

- A novel tele-operation system for the medical application have been proposed, and the tele-operation controller in the system also have been designed.
- A novel kind of wireless hybrid microrobot with gravity compensation mechanism have been designed.
- The control algorithm of 8-Steps rotation magnetic field have been proposed to improve the quality of rotation magnetic field.
- Some experiments have been taken to verify the feasibility of the 8-Steps control algorithm and the tele-operation system.

Keywords

Tele-operation, Wireless microrobot, Hybrid motion, External magnetic field

1. Introduction

Gastrointestinal tract driven by microrobot actively is expected in the diagnosis, treatment, spraying, sampling and other medical engineering while MEMS (micro-electromechanical systems) technology is combined with the medical technology and application, which will play an important role in the clinical application [1, 2]. Wireless microrobots are employed in a wide range of biomedical application. For example, they may be used for microsurgery in blood vessels, which is expected to become an increasingly widely adopted medical procedure in the near future. With advances in precision processing technology, several types of microrobots have been developed for various applications and further progress in this field is expected. They have many potential to accomplish many medical procedures radically. The microrobots are both safe and reliable, and they can be carried deeply within the body of living organisms to perform tasks [3].
As the size limitation of the microrobot, the actuation part including the power source is difficult to integrate into the microrobot. Therefore, several actuation mechanisms have been developed and used to propel the microrobot from a remote site, which are used for providing locomotion in the pipe such as piezoelectric elements [4, 5], air cylinders [6], electrorheological fluids [7], shape memory alloys [8, 9], electromagnetic motors [10-14], and globular magnetic actuator capable of locomotion in a pipe by combination of mechanical vibration and electromagnetic force [15, 16]. Honda developed a new kind of wireless swimming robot with a tail fin which can swim in one direction [17]. Thereafter Mei Tao developed another kind of wireless microrobot with desirable experiment results by using a new kind of intelligent magnetic material FMP [18]. Nokata developed new magnetic rotational drive by use of magnetic particles with specific gravity smaller than a liquid [19].

As wireless drive to the microrobot is a key technique in medical engineering applications, and a magnetic microrobot which driven by the external magnetic field demonstrates the wireless operation. There is no battery, no controlling devices required in the body of the microrobot. Therefore, we will focus on the development of an electromagnetic actuation (EMA) system that uses an external magnetic field to produce the propulsion forces. With the different kinds of external magnetic field driven, there are many locomotion forms had been proposed, for example, the fish-like motion, [20], paddle motion [21], propeller-driven motion [22], spiral motion [23] and hybrid motion [24]. The team of Prof. Guo had studied on the wireless in-pipe microrobot that driven by the external magnetic field many years, many kinds of microrobot had been developed in recent year as shown in Fig. 1. This kind of the wireless microrobot driven was very suitable to human surgery or drug delivery because it had a small size and could work in long time [25].

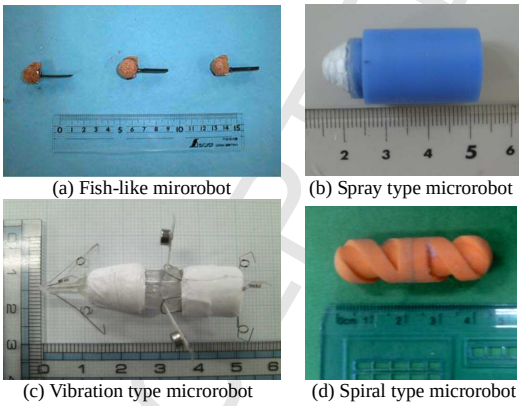

(a) Fish-like mirorobot (b) Spray type microrobot

(c) Vibration type microrobot (d) Spiral type microrobot

Fig.1.
Several kinds of wireless microrobots.

The control system has been proposed to realize the energy supply by wireless and flexibility movement. However, in the practical applications, many problems have emerged, such as the limitation of the magnetic flux density, the low security to the doctor and low practicability in the clinical. So in this paper, we propose a novel tele-operation control system, and the tele-operation controller has been designed to solve these problems we mentioned.

The structure of this paper is as following: Firstly, we will propose the novel tele-operation system, and then design the master controller and slave controller respectively in the system. Secondly, we will design the wireless microrobot with hybrid motion and analyze the motion mechanism of it. Thirdly, we will propose and design the control algorithm for the system. Some experiments and results for the system performance evaluation have been given in the fourth part. And the final part of the paper presents our conclusion and future work.

2. The Tele-operation System

2.1 Overview of the tele-operation system

A conceptual diagram of the tele-operation system was shown in Fig. 2. The system was divided into two main parts, which are the master side and the slave side. In the master side, the doctor could operate the Joysticks of the maser controller with viewing a monitor. The operating and state information was acquired and transmitted from the slave side. The slave controller would receive the control signals from the master controller through the wireless communication, and then the external magnetic field was adjusted to change the motion state of microrobot in the intestinal tract of patient. The information could be processed and integrated, which was from the X-ray detector, the microrobot and the magnetic array sensor respectively. Then the information would transmit to the master side through the Internet communication as the doctor's reference. The system made the doctors and patients separately, which would avoid the doctor working long time in the X-ray radiation, so that the safety of surgery could be improved.

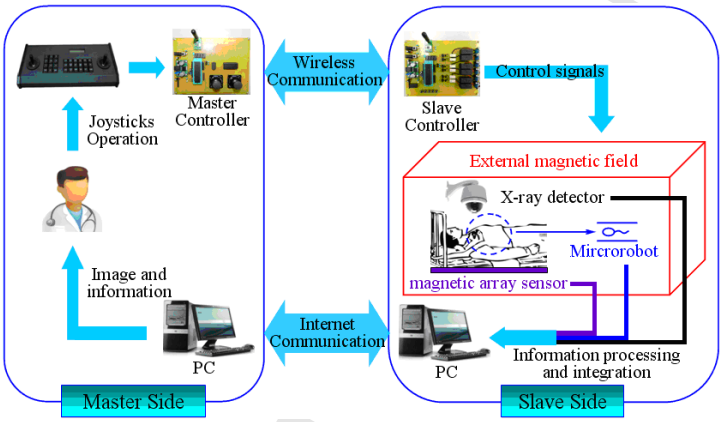

Fig.2.
The conceptual diagram of the tele-operation system.

2.2 Design of the master controller

In the system, the most significant part was the master controller and the slave controller. The main task of master controller was acquired and processed the location information of doctor operating joysticks, then sent control information to the slave controller. The main task of the slave controller was to receive the control information from the master controller through the wireless communication, then outputted the control signals to adjust the external magnetic field and change the motion state of the microrobot by selecting the corresponding control algorithm.

The diagram of our designed master controller was shown in the Fig. 3. In the operating room, the doctor could operate the Joysticks according to image of the microrobot in the intestinal tract, then location and status of the microrobot could be controlled by the master controller.

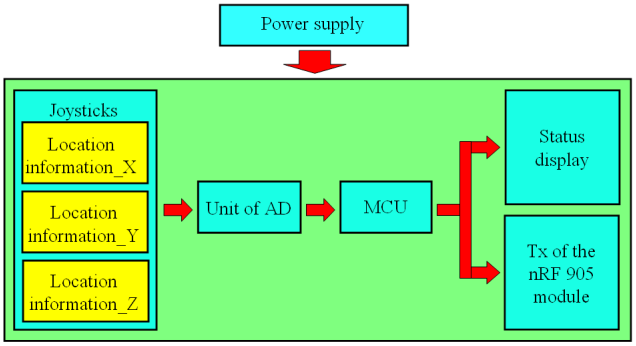

Fig.3.
The block diagram of the master controller.

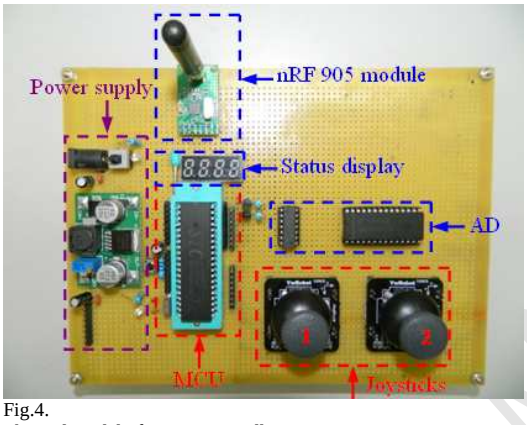

Fig.4.
The real model of master controller.

The real model of the master controller had been shown in the Fig. 4. In the master controller, joystick 1 could adjust the motion statue of microrobot in the x-axis and y-axis, and joystick 2 could adjust the motion statue of microrobot in the z-axis. The doctor could operate the joysticks to adjust the motion status of the microrotbot in real time. By the acquisition and processing of AD unit, the control information inputted the MCU of master controller. Then the LED would display the current motion status such as the velocity and moving direction of the microrobot, and the nRF 905 module would transmit the control information to the slave controller.

2.3 Design of the slaver controller

The slave controller was placed in the operation room, and output was connected with the external magnetic field model directly. It could call the corresponding control algorithms by referring to the control information which was transmitted from the master controller.

The diagram of our designed slave controller was shown in Fig.5. In the slave side, the current control mode including the manual control mode and the tele-operation control mode could be selected by doctor. In tele-operation control mode, the nRF 905 module could receive control information which was transmitted from master controller, and then inputted them into the MCU of slave controller. It could realize remote control in the real time, and the furthest transmission distance was about 500 m between the master side and the slave side.

Another manual control mode could be used in some special circumstances. For instance, the system was failure, the patient needed a rest in the operation, or the location of lesions had been found, the doctor needed to communicate the sickness with patient, and then identified the lesions further in the operation room by controlling the buttons of the slave controller.

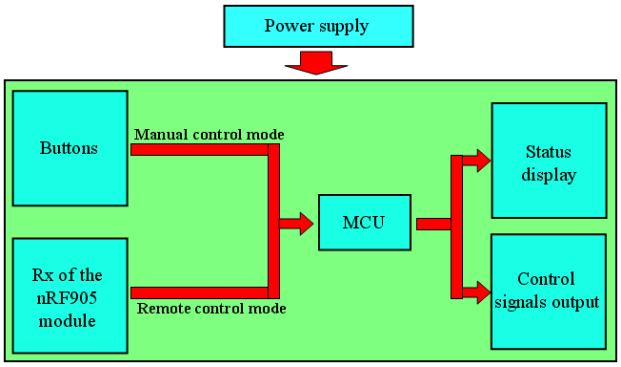

Fig.5.
The block diagram of the slave controller.

The real model of the slave controller had been shown in the Fig. 6. We could select the current control model by a button, the driving and control signals which flowing into the coils would be outputted by relay groups. Then the LED would display current motion status such as the velocity and moving direction of the microrobot.

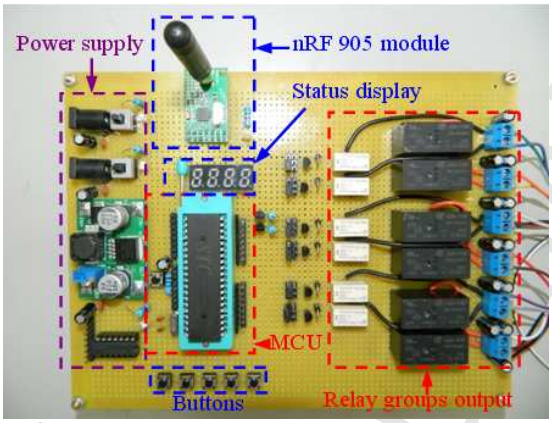

Fig.6.
The real model of slave controller.

3. Motion mechanism of the microrobot with hybrid motion

3.1 Structure of the hybrid motion microrobot

The hybrid structure of microrobot consisted of two main part: the part of spiral structure and the part of fish-like structure, which was shown in Fig. 7.

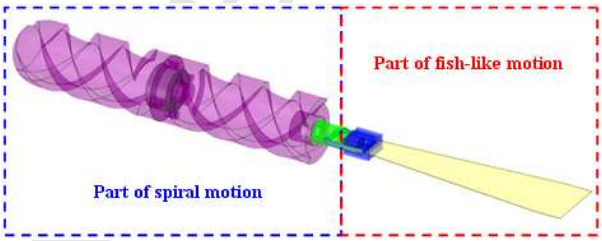

Fig.7.
Structure of the wireless microrobot with hybrid motion.

Many kinds of microrobots designed in the previous study were difficult to move in the vertical direction, which was mainly due to the weight of the microrobot. We considered the gravity

compensation mechanism to make the microrobot suffered by the force close zero in the vertical direction, when it was at rest. With the aided of 3D printing technology, the hybrid microrobot had been design, and the gravity compensation method could be used to make the microrobot suspended in the pipe as following [26].

When we designed the structure of the hybrid microrobot, the volume of each part could be obtained in many ways. According to the Archimedes Law, we could obtain the equations as:

$$\rho_{mix} = \rho_{liquid} \tag{1}$$

$$\begin{aligned} M_i &= m_i - m_j \\ &= \rho_{mix} V_i - m_j \\ &= \rho_{liquid} V_i - m_j \end{aligned} \tag{2}$$

where, ρ_{mix} is the mixed density of the hybrid microrobot, ρ_{liquid} is the density of the liquid in the pipe, m_i is the mass of each part, m_j is the mass of appertaining in each part, such as magnet and miniature bearing, V_i is the volume in each part we have obtained, M_i is the printing mass of each part.

We could select the percentage of filler during the 3D printing process then each mass of the printing part could be calculated. When the each mass of the printing part was equal to the M_i, the ρ_{mix} would be similar to the ρ_{liquid}, so the wireless microrobot could be suspended in the pipe in theory, which would improve the dynamic performance in the vertical direction.

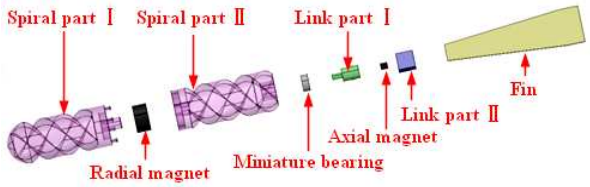

Fig.8.
Assembly diagram of the proposed hybrid microrobot.

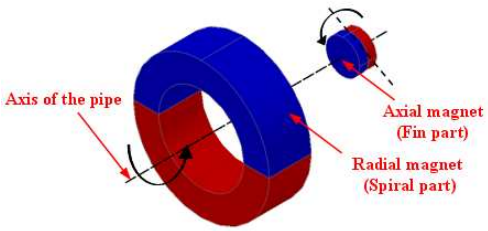

Fig.9.
Inner magnetic field in the hybrid microrobot.

Fig. 8 had shown the assembling process. We placed a piece of the radial magnet and the axial magnet to generate inner magnetic field in the microrobot which direction was perpendicular to each other as shown in Fig. 9. In this way, the spiral motion and fish-like motion could be controlled separately without any interference.

Compared with some microrobots designed in the previous study, the novel kind of wireless microrobot with hybrid motion had some advantages as following:
1) the microrobot was controlled by the external magnetic field wirelessly, which could improve the safe in the detection process.
2) the microrobot designed to bionics as a starting point, so it was suitable to the gastrointestinal detection well, and the bionic prototype was flagella.
3) the motion forms that spiral motion and fish-like motion could be changed by adjusting the external magnetic field.

4) the state of microrobot motion, which including the direction of motion and the velocity, could be adjusted by external magnetic field in real time.
5) the application of gravity compensation mechanism could improve the performance of microrobot in the motion, especially in the vertical direction.

We had designed two types of hybrid microrobot that with the different spiral unit numbers, in addition, they were also designed with the gravity compensation mechanism by 3D printing technology as shown in Fig. 10, and the designed parameters were shown in Table 1. They would be used for evaluating and comparing the performance in the experiments part.

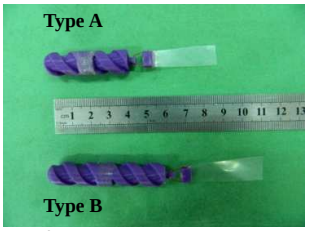

Fig.10.
Prototype of the proposed microrobots.

Table 1.
Specification of the microrobots.

	Type A	Type B
Size of the body (mm)	90	110
Size of the spiral part (mm)	Φ10 × 40	Φ10 × 60
Size of the fin part (mm)	40 × 10 × 0.125	
Spiral unit number	3	4
Size of radial magnet (mm)	Φ7.8 × Φ4 × 4	
Size of axial magnet (mm)	Φ2× 2	
Size of miniature bearing (mm)	Φ5 × Φ2 × 1	

3.2 External magnetic field model

In the external magnetic field model, there were two pairs of coils, which as shown in Fig. 11. In order to enhance the density of magnetic field, we embedded the magnetic cores. The specification of each coil had been given in Table 2.

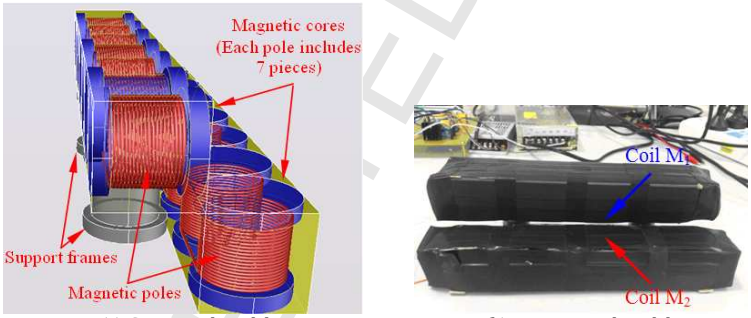

(a) Conceptual model (b) Experimental model

Fig.11.
Assembly diagram of the proposed hybrid microrobot.

Table 2.
Specification of each coil.

	Coil M_1	Coil M_2
Turns per coil (times)	150	150
Wire diameter (mm)	0.2	0.2
Length × Width × Height (mm)	210 × 30 × 35	210 × 30 × 35
Resistance (Ω)	10.2	10.4
Size of magnetic core (mm)	Φ30 × 35	Φ30 × 35
Magnetic core (piece)	7	7

Following the Biot-Savart Law, the relationship between the magnetic flux density H and current i had been measured by a gauss meter as shown in Fig. 12, and (3) of the curve could be fitted as well.

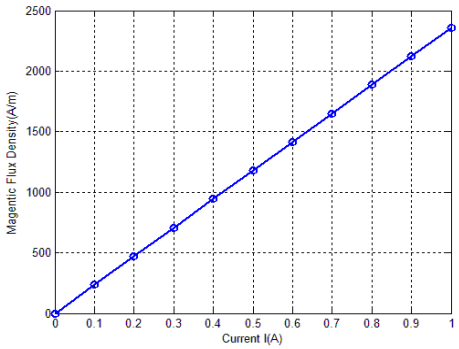

Fig.12.
Relationship between the magnetic flux density and current.

$$H(i) = 2.357 \times 10^3 \times i \tag{3}$$

3.3 Fish-like motion

The fish-like motion could be realized by the alternating magnetic field model. We just needed input the control signal to any a pair of coils as shown in Fig. 13.

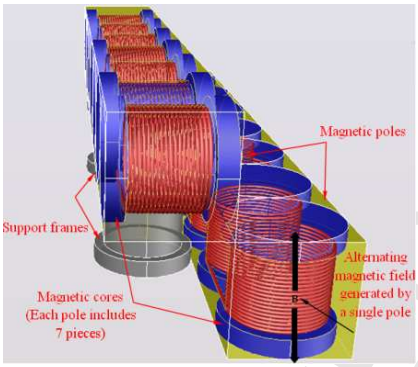

Fig.13.
The alternating magnetic field model.

Ampere's law related the circulation of B around a closed loop to the current flux through the loop as following:

$$\oint_L \vec{B} \cdot d\vec{l} = \oint_L B\cos\theta \cdot dl = \oint_L \frac{\mu_0 I}{2\pi r} r d\varphi = \frac{\mu_0 I}{2\pi}\int_0^{2\pi} d\varphi = \mu_0 I \tag{4}$$

where, B is the magnetic flux density, l is the length of the coil, r is the radius of the coil, μ_0 is the permeability of vacuum, I is the current in coil.

And the magnetic torque T acting on the permanent magnet in the external magnetic field H was given by:

$$T = M \times H \tag{5}$$

where, M is the magnetic moment of the permanent magnet.

3.4 Spiral motion

The spiral motion could be realized by the rotation magnetic field model. We should input the

control signals to the two pairs of coils which had same amplitude, but the phase difference of 90 degrees as shown in Fig. 14.

Then the magnetic flux density generated by coil M_1 and M_2 could be given by:

$$B_1 = B_{10} \sin \omega t \tag{6}$$

$$B_2 = B_{20} \sin\left(\omega t + 90^\circ\right) \tag{7}$$

In order to analyze the magnetic field convenient, we assumed $B_{10}=B_{20}=B_0$. The rotation vector directions of B_1 and B_2 were perpendicular to each other, so the absolute value and the direction of the magnetic field after the superposition of the two magnetic field vectors were:

$$B = \sqrt{B_1^2 + B_2^2} = \sqrt{(B_0 \sin \omega t)^2 + (B_0 \cos \omega t)^2} = B_0 \tag{8}$$

$$\tan\theta = B_1 / B_2 = \tan \omega t \tag{9}$$

From the equation (8) and equation (9), we could find the value of the synthesis magnetic field strength is a constant, and it was equal to the maximum value B_1 (or B_2). Besides that, the direction of B was along with the time changing periodically. So the synthesis vector B was a rotation vector, and the angular velocity of rotation was ω, which was a rotation magnetic field.

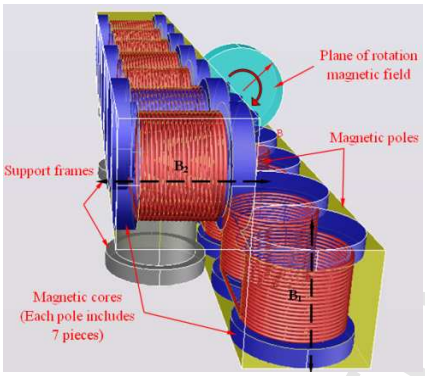

Fig.14.
The rotation magnetic field model.

The propulsive force and torque was provided by rotation magnetic field and could be changed as (10) and (11) [27]:

$$T = \mu_0 VM \times H = VM \times B \tag{10}$$

$$F = \mu_0 V(M \cdot \nabla) \times H = V(M \cdot \nabla) \times B \tag{11}$$

where, V is the volume of the body, ∇ represents a gradient operator.

4. Control algorithm

4.1 Analysis of the external magnetic field motion

The motion mechanism of the microrobot was related to the external magnetic field model. We could change the motion form of the wireless microrobot by adjusting the input current signals as shown in Fig. 15.

Due to the spiral motion could not only obtain the maximum driving force, but also was the highest efficiency in a very small space, so we would focus on the study of this kind of motion.

When two input currents flowing into the coils, a rotation magnetic field could be generated, and the kinematic characteristic of microrobot was shown in Fig. 16. The permanent magnet would rotate following the rotation magnetic field. With the spiral structure, it could move forward. By changing the order of two-phase input currents, the opposite direction of rotation magnetic field could be obtained immediately. Then the microrobot would obtain an opposite direction of the propelled force and moved towards the opposite direction. The velocity of microrobot could be controlled by adjusting the frequency of input current signals [28].

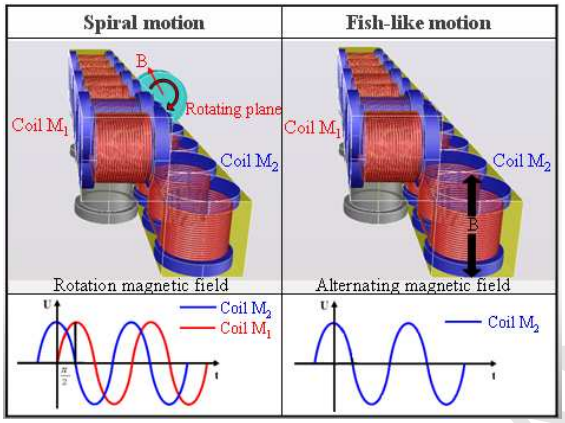

Fig.15.
Input current signals.

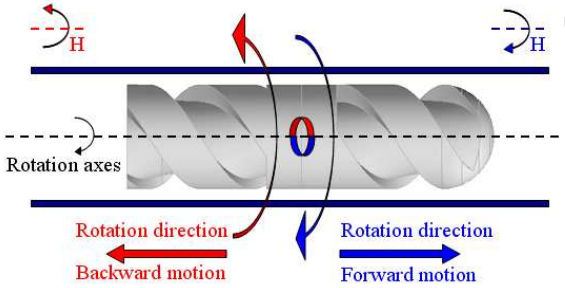

Fig.16.
Kinematic characteristics of the proposed microrobot.

4.2 Control algorithm of 8-Steps rotation magnetic field

In the tele-operation system, we utilized the relay output method instead of traditional power amplifier chips. Due to the relay could just output square wave signal, the rotation magnetic field was not very uniform. So we also proposed the control algorithm of 8-Steps rotation magnetic field to improve the quality of rotation magnetic field which was generated by the relay groups.

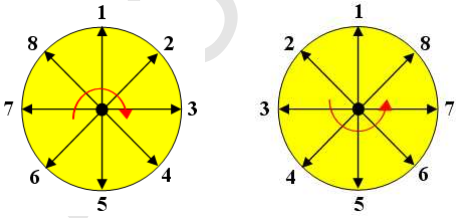

(a) Clockwise rotation (b) Counter Clockwise rotation

Fig.17.
8-Steps rotation plane.

The movement of the wireless microrobot was controlled by a rotation plane which was shown in the Fig. 17. We had chosen eight special vectors of the rotation plane in a circle, and then the either direction of magnetic field vectors would be designed and obtained by the relay groups. So a more uniform rotation magnetic field could be generated.

Each relay group consisted of two pieces of relays that could output four kinds of control signals, which was shown in the Fig. 18.

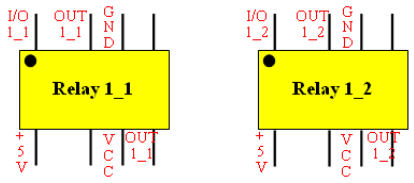

(a) Relay group

I/O 1_1	I/O 1_2	OUT 1_1	OUT 1_2	Output
0	0	1	1	×
0	1	1	0	+Vcc
1	0	0	1	-Vcc
1	1	0	0	0

(b) Truth table

Fig.18.
Function analysis of relay group.

The clockwise rotation could be obtained as shown in Table 3, and the opposite direction of rotation also could be obtained from the Step ⑧ to ①. By outputting the I/O signals from controller, a rotation magnetic field could be generated.

Table 3
8-Steps rotation magnetic field.

Step	①	②	③	④	⑤	⑥	⑦	⑧
Vector	↑	↗	→	↘	↓	↙	←	↖
OUT 1_1	↑ 01	↑ 01	— 11	↓ 10	↓ 10	↓ 10	— 11	↑ 01
OUT 1_2	— 11	→ 01	→ 01	→ 01	— 11	← 10	← 10	← 10
I/O	0xfd	0xf5	0xf7	0xf6	0xfe	0xfa	0xfb	0xf9

The control signals outputted by the relay groups were shown in the Fig. 19.

With this method and control algorithm, many advantages could be concluded as following:
(a) the signals outputted by relay groups, which would reduce the heat generated in the circuit greatly.
(b) the quality of rotation magnetic field could be improved by 8-Steps control algorithm.

(c) the bipolar drive signals could be outputted by a unipolar power, so the requirement and cost of power supply would be reduced.
(d) the magnetic field intensity would be enhanced, which was due to we could use a high unipolar power supply easily without considering the circuit heating problem.

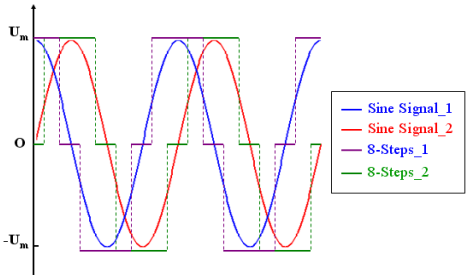

(a) Spiral motion

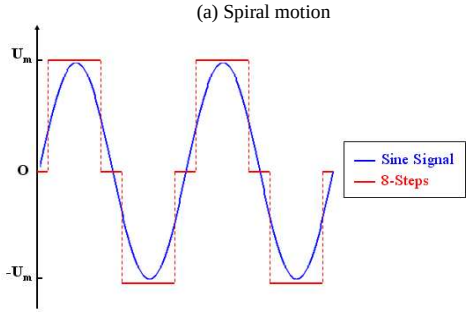

(b) Fish-like motion

Fig.19.
Contrast control signals.

5. Experiments and results

In the detection process, the wireless microrobot should complete basic motion in the pipe, such as forward-backward motion and upward-downward motion. Based on the theoretical analysis of the designed microrobot in our previous study, we made several experiments to evaluate the performance of the tele-operation system. The experimental system of was shown in Fig. 20 and Fig. 21, and the average velocity of the wireless microrobot could be measured by a laser displacement sensor (KEYENCE IL-100). We used a tube to simulate the intestinal tract, and the properties and characteristics of pipeline were shown in the Table 4.

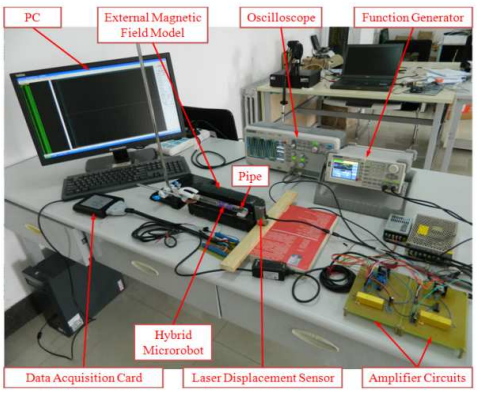

(a) Horizontal direction

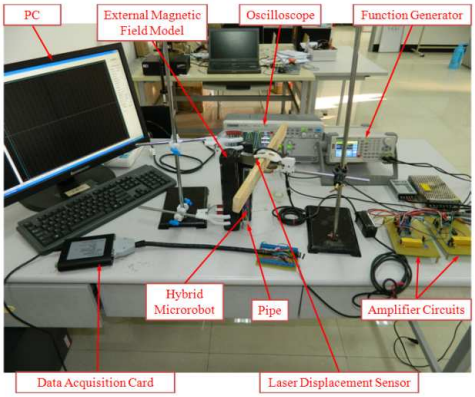

(b) Vertical direction

Fig20.
Experimental system of traditional power amplifier chips.

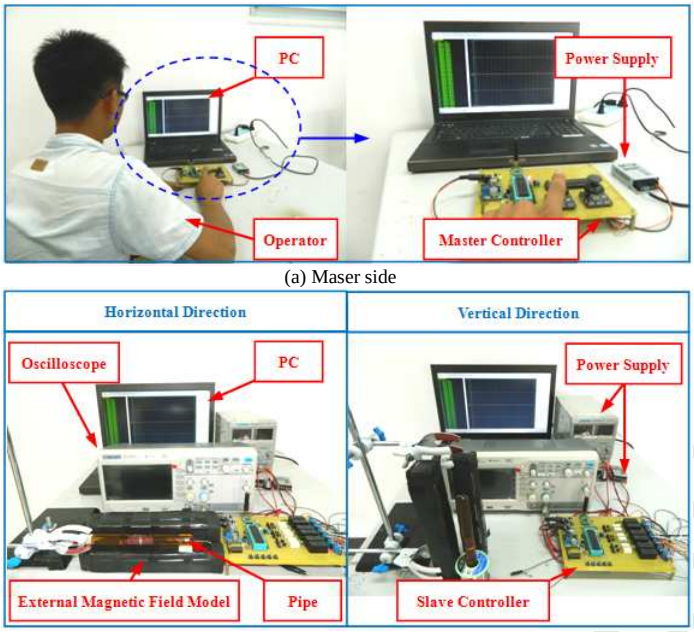

(a) Maser side

(b) Slave side

Fig.21.
Experimental system of tele-operation system.

Table 4.
Properties and characteristics of pipeline.

Material	Glass
Size (mm)	Φ12 × 20
Coefficient of friction	0.7

5.1 Experiment on the performance evaluation

The experiments on the spiral motion, including the forward-backward, upward-downward motion had been taken. We carried out the experiments by adjusting frequency of the input currents from 0 Hz to 20 Hz in real time, and the amplitude of input currents was fixed at 0.7 A. The rotation magnetic field generated by the sine wave signals and 8-Steps square wave signals respectively, the relationship between the velocity of the hybrid microrobot (Type A) and frequency of the rotation magnetic field could be obtained as shown in the Fig. 22.

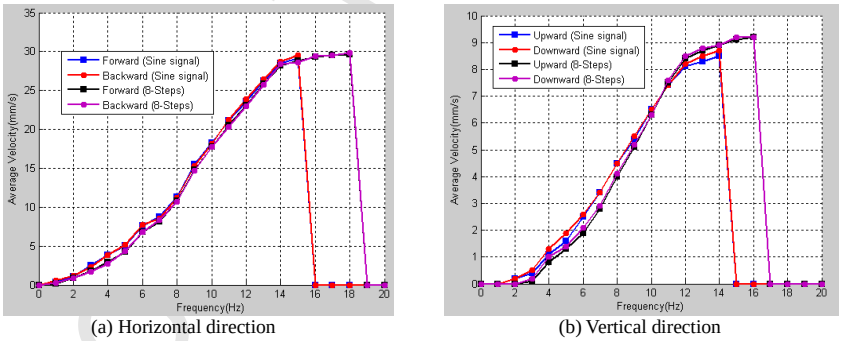

(a) Horizontal direction

(b) Vertical direction

Fig.22.
Experimental system of the spiral motion.

Viewing from the experimental results in Fig. 22, it indicated that the microrobot with gravity compensation owned the similar dynamic characteristics in the movement, and could realize forward-backward, upward-downward motion in the pipe [29]. The available frequency band with

the control algorithm of 8-Steps rotation magnetic field was much wider than the sine signals, and the microrobot could still keep moving at a high frequency band. In addition, we could find the velocity of the microrobot declined to zero at the region of high level frequency. It was because when the applied magnetic field rotated faster than the microrobot's step-out frequency (the frequency requiring the entire available magnetic torque to maintain synchronous rotation), the velocity of the microrobot dramatically declined when operated above the step-out frequency [30]. Based on the tele-operation system, the maximum velocity of the wireless microrobot also had been obtained at 29.8 mm/s round 18 Hz in the horizontal direction and 9.2 mm/s round 16 Hz in the vertical direction with input current of 0.7 A.

According to our previous study, the fish-like motion just could move towards a single direction. By changing the input signals, the magnetic field model generated the alternating magnetic field, and then the hybrid microrobot switched to the fish-like motion. We chose the best design parameters of the fin part as shown in Table 1, which according to the results of previous study. Then we carried out the experiments by changing the frequency of input currents from 0Hz to 30Hz, and the amplitude of input currents were fixed at 0.7A. The average velocity of hybrid microrobot (Type A) had been obtained in Fig. 23. The maximum velocity of the wireless microrobot had been obtained at 9.6 mm/s round 16 Hz in the horizontal direction.

Comparing the experimental results in Fig. 22 and Fig. 23, we could conclude that spiral structure could produce greater propulsion in the moving process, so the dynamic characteristic of the spiral motion was superior to the fish-like motion. Beside that, the fin part could reduce the shock of the spiral part and made its movement more smoothly.

By the experiments, the feasibility of the 8-Steps control algorithm and the tele-operation system also had been verified, so it could replace the sine wave signals and power amplifier chips effectively.

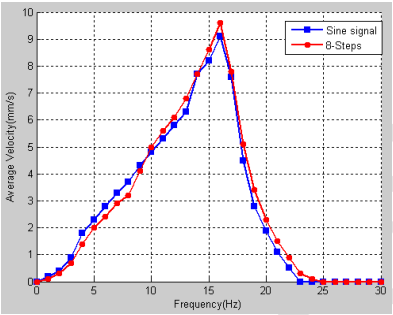

Fig.23.
Experimental result of the fish-like motion.

5.2 Performance comparison experiment

We designed two types of hybrid microrobot (Type A and Type B) as shown in Fig. 10, which only had the difference on spiral unit number. The modeling analysis and performance evaluation of spiral motion part had been discussed in the previous study [29]. Based on the tele-operation system was shown in Fig. 21, the average velocity of the horizontal direction and vertical direction could be obtained as shown in Fig. 24.

From the experimental results, we could conclude that Type A and Type B had the same dynamic trend of movement. Due to Type B had more spiral unit number, and it could obtain greater driving force at the high frequency band, so with a higher maximum velocity. However, the weight of Type B was much heavier than Type A, it needed a greater starting torque, so the velocity of Type B was a little lower than Type A at the low frequency band. Moreover, when the hybrid microrobot was in high-speed rotation motion, the Type B would need more kinetic energy, so the cutoff frequency of Type B was much lower than Type A.

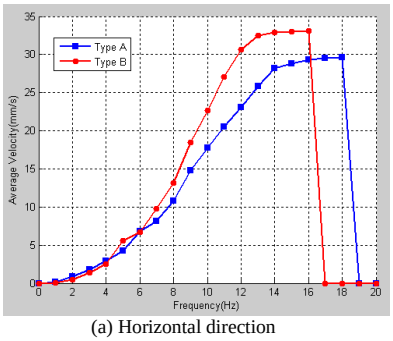

(a) Horizontal direction

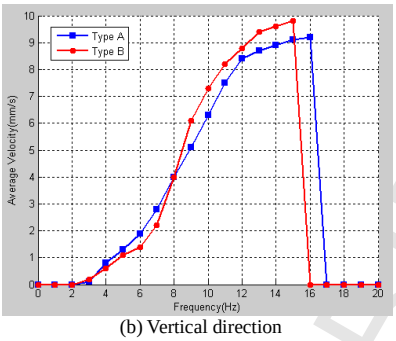

(b) Vertical direction

Fig.24.
Experimental result of the performance comparison.

5.3 Experiment on different amplitudes of input currents

From (10) and (11), we could obtain the propulsive force and torque provided by the external magnetic field was related with the amplitudes of input currents. So we made another experiment to evaluate the effect between the dynamic performance and the amplitudes of input currents.

Based on the tele-operation system, we could change amplitudes of input currents by adjusting the power supply. Due to the external magnetic field model had two coils, and the resistance of the coils was very similar, so the input currents could be calculated as:

$$I_{Coil\_1} = I_{Coil\_2} = \frac{I_{in}}{\sqrt{2}} \tag{12}$$

where, I_{Coil_1}, I_{Coil_2} are the currents' amplitude flowing into the coil 1 and coil 2, I_{in} is the currents' amplitude outputted by the power supply.

We selected the currents' amplitude outputted by the power supply as 1A, 2A and 3A respectively, then the currents' amplitude flowing into the coil 1 and coil 2 could be calculated as 0.7A, 1.4A and 2.1A. The experimental temperature was fixed the room temperature (about 20 □), and results were shown in Fig. 25.

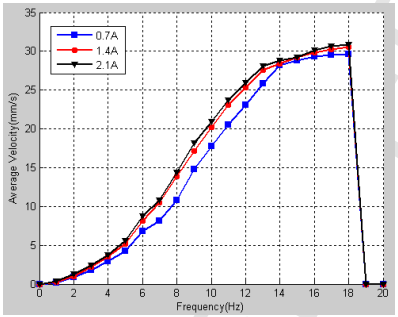

(a) Spiral motion in horizontal direction

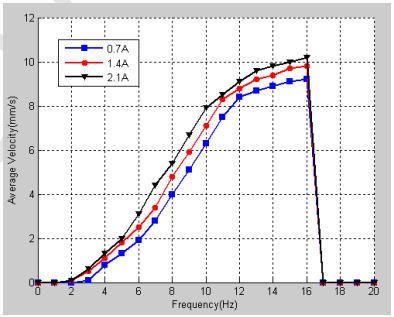

(b) Spiral motion in vertical direction

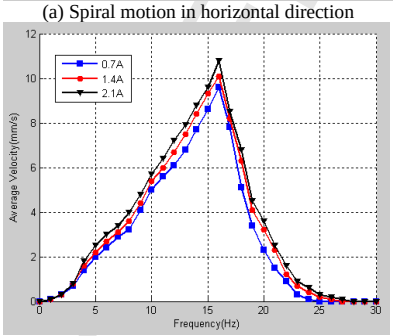

(c) Fish-like motion

Fig.25.
Experimental result of the effect on different input currents' amplitude.

From the experimental results, we could conclude that the dynamic trend of movement with different input currents' amplitude was similar, and the average velocity of the wireless microrobot was much faster when the input currents' amplitude was higher. However, the phenomenon of the core heat was more obvious when amplitude of input currents was higher, so we should select a suitable and applicable value of currents' amplitude in the actual operation.

5.4 Experiment in different liquids

In the process of clinical operation, the intestinal fluid of each patient was different, so we made an experiment on the performance evaluation of different liquids [31].

Re was defined by the following equation:

$$\mathrm{Re} = \frac{Vd}{\upsilon} = \frac{\rho V d}{\mu} \tag{13}$$

where, V is representative velocity, d is diameter of the pipe, υ is kinematic viscosity of the liquid, ρ is density of the liquid, μ is viscosity of the liquid.

The propulsive force was the sum of the drag force vectors in the direction of movement as in equation:

$$F_d = \frac{1}{2} C_d(\mathrm{Re}) \rho V^2 A \tag{14}$$

where, C_d is drag coefficient based on wetted surface area A, ρ is the density of the liquid.

The parameter C_d was related to Re, the relationship between the Re and C_d as shown in Table 5. So Re was related to the density and viscosity of liquid in the experiment and it was a significant parameter, which would effect on the kinematic characteristics of the microrobot in pipe. In this experiment, we chose two kinds of liquids that distilled water and oil in the experiment, and the specification of each liquid was shown in the Table 6.

Table 5.
Relationship between Re and C_d.

Re	**C_d**
$\mathrm{Re} \leq 10^3$	20.4/Re
$10^3 < \mathrm{Re} < 10^5$	0.40
$\mathrm{Re} \geq 10^5$	0.10

Table 6.
Specification of each liquid.

Kind of liquid	**Viscosity μ (Pa•S)**	**Density ρ (10^3 kg/m^3)**	**Temperature (℃)**
Distilled water	1.005×10^{-3}	1	20
Oil	0.95	0.935	20

Based on tele-operation system, the average velocity of the wireless microrobot (Type A) had been measured, and the amplitude of input currents was fixed at 0.7 A. The experimental result was shown in Fig. 26.

From the experimental result, we could conclude that the dynamic trend of movement in the distilled water and oil was similar, and the average velocity of the wireless microrobot in distilled water was much faster than in the oil. It was because the viscosity of the oil was larger than distilled water and the F_d in (14) was much larger when the microrobot moving in the oil.

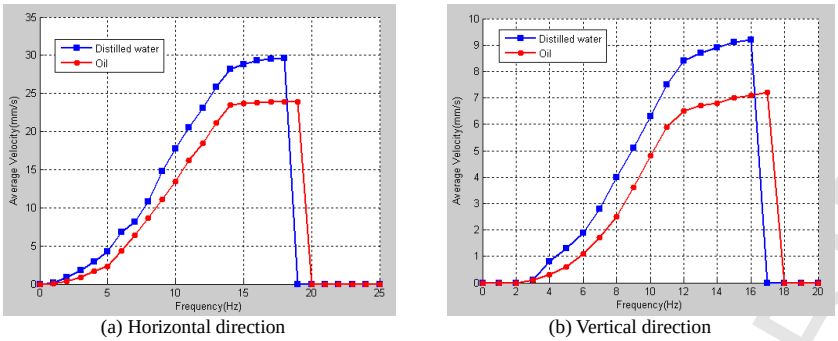

(a) Horizontal direction (b) Vertical direction

Fig.26.
Experimental result of the motion in different liquid.

In order to selecting velocity of the wireless microorbot in real time, we also fitted the curves of the velocity in the horizontal and vertical direction as shown in Fig. 27, and the fitting equations could be obtained as shown in (15) - (18). So the velocity could be controlled by adjusting the frequency of input currents accurately in the practical application.

$$V_{Distilled\ \ water\_H} = -0.016 f^3 + 0.4356 f^2 - 1.0715 f + 0.7938 \quad (15)$$

$$V_{Oil\_H} = -0.0139 f^3 + 0.3896 f^2 - 1.1948 f + 0.7268 \quad (16)$$

$$V_{Distilled\ \ water\_V} = -0.008 f^3 + 0.1997 f^2 - 0.6001 f + 0.2673 \quad (17)$$

$$V_{Oil\_V} = -0.0064 f^3 + 0.1672 f^2 - 0.6080 f + 0.3228 \quad (18)$$

where, $V_{Distilled\ water\_H}$, $V_{Distilled\ water\_V}$ are the velocity of horizontal and vertical direction in the liquid of distilled water, V_{Oil_H}, V_{Oil_V} are the velocity of horizontal and vertical direction in the liquid of oil, and f is the frequency of input currents.

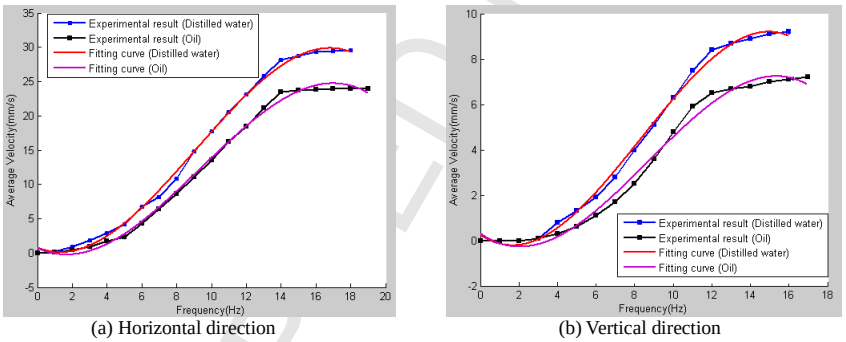

(a) Horizontal direction (b) Vertical direction

Fig.27.
Fitting curves of the velocity.

6. Conclusion and future work

In this paper, a novel tele-operation system for the medical application had been proposed, and we also designed the tele-operation controller in the system which was including the master controller and slave controller. Then a novel kind of wireless microrobot with hybrid motion also had been designed. We had discussed design method and gravity compensation mechanism of the hybrid microrobot. By changing the input signals of magnetic field model, the spiral motion and fish-like motion could be switched immediately. In order to generate a more uniform rotation magnetic field to control the motion of the wireless microrobot, we proposed the control algorithm of 8-Steps rotation magnetic field for the controller.

Based on some experiments, the feasibility of the 8-Steps control algorithm and the tele-operation system had been verified, so it could replace the sine wave signals and power amplifier chips effectively. We also evaluated the performance including the microrobot with different spiral number, the outputted signals with different amplitudes of input currents and the movement of microrobot in different liquids. In addition, the curves of the velocity in the horizontal and vertical direction were also fitted well. The experimental results could be concluded as following:

(1) The hybrid wireless microrobot with gravity compensation owned the similar dynamic characteristics in the movement, and it could realize forward-backward, upward-downward motion in the pipe.
(2) The available frequency band with the control algorithm of 8-Steps rotation magnetic field was much wider than the sine signals, and the microrobot could still keep moving at a high frequency band.
(3) The dynamic characteristic of the spiral motion was superior to the fish-like motion. Beside that, the fin part could reduce the shock of the spiral part and made its movement more smoothly.
(4) The wireless microrobot (Type B) with more spiral number could obtain a higher maximum velocity than microrobot (Type A), but available frequency bandwidth of the microrobot (Type B) movement was a little smaller than microrobot (Type A).
(5) The average velocity of the wireless microrobot was much faster when the input currents' amplitude was higher.
(6) The average velocity of the wireless microrobot in distilled water was much faster than in the oil.

The experimental results showed a good performance on our designed tele-operation controller, and it had many advantage. For example, the signals outputted by relay groups could reduce the heat generated in the circuit greatly, the quality of rotation magnetic field could be improved by 8-Steps control algorithm, the requirement and cost of power supply would be reduced, which was because the bipolar drive signals could be outputted by a unipolar power, the magnetic field intensity would be enhanced.

In the future, we will focus on optimal the tele-operation system, including establish a more flexible external magnetic field platform such as the 3 axes Helmholtz coils, and realize the more DOFs movement in pipe. The tele-operation system and the wireless microrobot with hybrid motion would be widely used in medical clinic field.

Acknowledgments

This research is supported by National High Technology Research Development Plan (863 Plan: 2015AA040102) and General Research Program of the Natural Science Foundation of Tianjin (13JCYBJC38600) and the Project-sponsored by SRF for ROCS, SEM and Key Research Program of the Natural Science Foundation of Tianjin (13JCZDJC26200).

References

[1] H Saito, K Sato, K Kudo and K. Sato, "Fundamental study of mover travel inside a small diameter pipe", International Journal of Mechanical Engineers, Vol. 66, No. 641, pp.346–353, 2000.
[2] H Choi, K Cha, J Choi, et al. "EMA system with gradient and uniform saddle coils for 3D locomotion of microrobot", International Journal of Sensors and Actuators A: Physical, Vol. 163, No. 1, pp.410-417, 2010.
[3] P Swain, "The future of wireless capsule endoscopy", World Journal of Gastroenterology. Vol. 14, No. 26, pp. 4142, 2008.
[4] H. Saito, K. Sato, K. Kudo and K. Sato, "Fundamental study of mover travel inside a small diameter pipe", Journal of Mechanical Engineers, Vol. 66, No. 641, pp. 346–353, 2000.

[5] J. Fujita, Y. Shiraogawa, S. Yamamoto and T. Kato, “Study of mobile mechanism with elastic fibers by using vibration”, Journal of Nippon Kikai Gakkai Ronbunshu C Hen. Vol. 70, No. 698, pp. 22–26, 2004.
[6] M. Ohno, T. Hamano and S. Kato, “Modeling and fabrication of a mobile inspection microrobot driven by a pneumatic bellows actuator for long pipes”, Journal of Robotics and Mechatoronics, Vol. 18, No. 1, pp. 11–17, 2006.
[7] Y. Kondo and S. Yokota, “Fluid power systems involving the use of an electro-rheological fluid”, Journal of Society of Mechanical Engineers, Vol. 64, No. 617, pp. 300–306, 1998.
[8] J. Kwon, S. Park, B. Kim and J. Park, “Bio-material property measurement system for locomotive mechanism in gastro-intestinal tract”, Proceedings of the 2005 IEEE International Conference on Robotics and Automation, pp. 1315–1320, 2005.
[9] D. Reynaerts, J. Peilw and H. Brussel, “Design of a shape memory actuated gastrointestinal intervention system”, Journal of Eurosensors, pp. 1181-1184,1996.
[10] Y Zhang, H Xie, N Wang, “Design, analysis and experiments of a spatial universal rotating magnetic field system for capsule robot”, Proceedings of 2012 IEEE International Conference on Mechatronics and Automation, pp. 998-1003, 2012.
[11] T. Miyagawa and N. Iwatsk, “Moving characteristics in bent pipes of in-pipe mobile robot with wheel drive mechanism using planetary gear drive”, Journal of Japan Society for Precision Engineering, Vol. 74, No. 12, pp. 1346–1350, 2008.
[12] J. Bocko, M. Kelemen, T. Kelemenova and J. Jezny, “Wheeled locomotion inside pipe”, Journal of Bulletin of applied mechanics, Vol. 5, No. 18, pp. 34–36, 2009.
[13] H. Choi and S. Roh, “In-pipe robot with active steering capability for moving inside of pipelines”, Journal of Bioinspiration and Robotics, Vol. 23, pp. 375–400, 2007.
[14] K. Suzumori, S. Wakimoto and M. Tanaka, “In pipe inspection micro robot adaptable to changes in pipe diameter”, Journal of Robotics and Mechatronics, Vol. 15, No. 6, pp. 609-615, 2003.
[15] H. Yaguchi and N. Sato, “Globular magnetic actuator capable of free movement in a complex pipe”, Journal of Magnetics, Vol. 46, No. 6, pp. 1350–1355, 2010.
[16] H. Yaguchi, N. Sato and A. Shikoda, “Magnetic actuator group of globular type capable of free movement in a complex pipe”, Journal of Magnetics, Vol. 47, No. 10, pp. 4159–4162, 2011.
[17] T Honda, T Sakashita, K Narahashi, et al. “Swimming properties of a bending-type magnetic micro-machine”. Journal of Magnetics Society of Japan, Vol. 25, Nos. 4(2), pp.1175-1178, 2001.
[18] T Mei, Y Chen, G Fu and D Kong, “Wireless Drive and Control of a Swimming Microrobot”, Proceedings of the 2002 IEEE International Conference on Robotics and Automation, Vol.2, pp.1131-1136, 2002.
[19] M Nokata, H Masuka, S Kitamura, “New magnetic rotational drive by use of magnetic particles with specific gravity smaller than a liquid”, Proceedings of the 2010 IEEE International Conference on Robotics, pp.2177-2182, 2010.
[20] S Guo, Q Pan, M B Khamesee, “Development of a novel type of microrobot for biobiomedical application”, Journal of Microsystem Technologies, Vol.14, No.3, pp.307-314, 2008.
[21] Q Pan, S Guo, “A Paddling type of microrobot in pipe”, Proceedings of the 2009 IEEE International Conference on Robotics and Automation pp.2995-3000, 2009.
[22] S Guo, Q Pan, “Mechanism and Control of a Spiral Type of Microrobot in Pipe”, Proceedings of the 2008 IEEE International Conference on Robotics and Biomimetics, pp.43-48, 2008.
[23] T Okada, S Guo, Q Fu, “A wireless microrobot with two motions for medical applications”, Proceedings of the 2013 ICME International Conference on Complex Medical Engineering, pp.306-311, 2012.
[24] Q Pan, S Guo and T Okada, “A Novel Hybrid Wireless Microrobot”, International Journal of Mechatronics and Automation, Vol.1, No.1, pp.60-69, 2011.
[25] J Guo, S Guo, X Wei, et al. “Development of a Wireless Endoscope with Symmetrical Motion Characteristics”, International Journal of Advanced Robotic Systems, DOI: 10.5772/58925, Vol. 11, pp. 1-13, 2014.
[26] S Guo, X Wei, J Guo, et al. “Development of a Novel Wireless Microrobot in-pipe with Hybrid Motion”, Proceedings of 2014 IEEE International Conference on Mechatronics and Automation, pp.1613-1618, 2014.

[27] J Guo, X Wei, S Guo, et al. “Performance Evaluation of the Wireless Microrobot in pipe with Symmetrical Spiral Structure”, Proceeding of the 2014 IEEE International Conference on Robotics and Biomimetics, pp.1252-1257, 2014.
[28] J Guo, S Guo, X Wei, et al. “Development of a New Kind of Magnetic Field Model for Wireless Microrobots”, Proceedings of the 2013 ICME International Conference on Complex Medical Engineering, pp.580-585, 2013.
[29] S Guo, X Wei, J Guo, et al. “Development of a Symmetrical Spiral Wireless Microrobot in Pipe for Biomedical Applications”, Proceeding of 2014 IEEE International Conference on Robotics and Automation, pp.4705-4710, 2014.
[30] A W. Mahoney, N D. Nelson, K E. Peyer, “Behavior of rotating magnetic microrobots above the step-out frequency with application to control of multi-microrobot systems”, Journal of Applied Physics Letters, Vol. 104, No. 14, pp .144101, 2014.
[31] K Ishiyama, K 1; Aral; M Sendoh, and A. Yamazaki, “Spiral-type Micro-machine for Medical Applications”, Proceeding of 2000 International Symposium on micromechatronics and human science”, pp. 65-69, 2000.

Shuxiang Guo (S'93-M'95-SM'03) received the B.S. and the M.S. degrees in mechanical engineering from the Changchun Institute of Optics and Fine Mechanics,Changchun, China, in 1983 and in 1986, respectively, and the Ph.D. degree in mechano-informatics and systems from Nagoya University, Nagoya, Japan, in 1995. In 1995, he was a Faculty Member at Mie University, Mie, Japan and in 1998 at Kagawa University, Kagawa, Japan. Currently, he is a Professor with the Department of Intelligent MechanicalSystem Engineering at Kagawa University. He haspublished about 370 refereed journal and conference papers. His current research interests include microrobotics and mechatronics, microrobotics system for minimal invasive surgery, micro catheter system, micro pump, and smart material (SMA, ICPF) based on actuators. Dr. Guo received research awards from the Tokai Section of the Japan Society of Mechanical Engineers (JSME), the Tokai Science and Technology Foundation, and the Best Paper Award of the IS International Conference, Best Paper Award of the 2003 International Conference on Control Science and Technology and Best Conference Paper Award of IEEE ROBIO 2004, IEEE ICAL 2008 and IEEE ICIA 2011 ,IEEE ROBIO 2013 ,IEEE ICIA 2014, in 1997, in 1998, in 2000, in 2003, in 2004, in 2008 , in 2011, in 2013 and in 2014, respectively. He also received the Chang Jiang Professorship Award from Ministry of Education of China, in 2005, and was offered Thousand-Elite-Project in China. He is the founding chairfor IEEE International Conference on Mechatronics and Automation. And he is the editor in chief for International Journal of Mechatronics and Automation.

Jian Guo received the B.S. degree in information and computing science from Changchun University of Technology, China, in 2005, the M.S. and the Ph.D. degrees in intelligent machine system from Kagawa University, Japan, in 2009 and in 2012, respectively. Currently, he is an associate professor in Tianjin University of Technology, China. He researches on biomedical robots, such as wireless microrobots in pipe and robotic catheter systems for biomedical applications. He has published about 20 refereed journal and conference papers in the recent three years. Dr. Guo received Best Conference Paper Award of CME 2013 and IEEE ICIA 2014 in 2013 and in 2014, respectively.

Xiang Wei received the B.S. degree in automation from Tianjin University of Technology, China, in 2012. Currently, He is a postgraduate researcher in control science and engineering in Tianjin University of Technology, Tianjin. He will get the M.S. degrees in control science and engineering from Tianjin University of Technology in 2015, Tianjin. He researches on wireless in-pipe microrobot for medical application, such as the wireless microrobot which is driven by external magnetic field for industry and biomedical applications. His current research interests include the microrobot with symmetrical spiral structure, hybrid motion and the

tele-operation control system. He has published about 5 refereed journal and conference papers in the recent three years.

Jian Guo

Shuxiang Guo

Xiang Wei